Contributions of the electrostatic and the dispersion interaction to the solvent shift in a dye-polymer system, as investigated by hole-burning spectroscopy

L. Kador, S. Jahn, and D. Haarer
Physikalisches Institut and Bayreuther Institut für Makromolekülforschung (BIMF), Universität Bayreuth, Postfach 101 251, D-8580 Bayreuth, West Germany

R. Silbey
Department of Chemistry and Center for Materials Science and Engineering, Massachusetts Institute of Technology, Cambridge, Massachusetts 02139
(Received 20 November 1989)

Persistent spectral holes burned in the system octaethylporphin in poly(styrene) exhibit a symmetrical broadening varying in a linear fashion upon application of a static electric field. This effect is due to permanent electric-dipole moments induced in the dye molecules by the electric "matrix field." The average value of the dipole-moment difference μ between the excited and the ground state of the guest molecules, which can be deduced from the broadening, shows a distinct increase from the blue to the red edge of the inhomogeneous absorption band, thus reflecting the varying dye-matrix interaction for centers with different solvent shift. A detailed analysis of this variation in the framework of a microscopic theory, based on a recent publication by Laird and Skinner [J. Chem. Phys. **90**, 3274 (1989)], leads to the conclusion that the solvent shift of the absorption lines and also the μ variation across the inhomogeneous band is largely dominated by the dispersion interaction. The electrostatic contribution to the line shift is smaller by about 2 orders of magnitude.

I. INTRODUCTION

The frequencies of optical-absorption lines of dye molecules are influenced by the environment in which the molecules are embedded. In most cases, the absorption and fluorescence lines in solid matrices are therefore shifted with respect to the positions corresponding to their molecular vacuum transitions. This effect, which is called "solvent shift" or "gas-to-crystal shift" has been investigated theoretically by numerous authors (see, for instance, Refs. 1–5). In general, one categorizes four mechanisms contributing to the solvent shift of an electronic transition, namely the dispersion interaction, the mutual electrostatic polarization of the dye and the solvent molecules, and the interaction between their static electric dipole moments, depending upon the polar nature of the involved molecules. In some cases, the situation may be even more complicated when special interactions such as hydrogen bonding[6] or charge-transfer effects[7] are present. Even in the absence of these strong interaction mechanisms, solvent-shift values often amount to as much as several hundred inverse centimeters.

A direct consequence of the shift of electronic absorption lines due to the interaction with the surrounding matrix molecules is the phenomenon of inhomogeneous broadening.[8,9] Since virtually any real solid contains a certain amount of lattice imperfections, the embedded dye molecules experience different chemical surroundings so that their transition frequencies do not coincide but are subject to a distribution. This situation holds for transitions of various kinds, e.g., between nuclear-spin, electronic-spin, vibrational, and electronic energy levels. In the optical case, the width of an inhomogeneous distribution can range between a few tenths of an inverse centimeter in high-quality single crystals and several hundred inverse centimeters in amorphous solids, which are characterized by a total lack of long-range order. In the following, we will restrict ourselves to the case of electronic transitions of dye molecules in disordered materials.

In order to overcome the problem of inhomogeneous broadening and to achieve a resolution of the order of the homogeneous linewidth (i.e., the width of one individual molecular absorption line), a number of methods of nonlinear laser spectroscopy have been developed. They operate either in the time domain like two-pulse and accumulated photon echo or in the frequency domain like fluorescence line narrowing and persistent spectral hole burning.[10–14] The hole-burning method has the special virtue of creating a narrow persistent marker in the inhomogeneous band that indicates small shifts of the absorption lines with high optical resolution. Therefore, this technique has not only been used for determining homogeneous linewidths but also for investigating the effects of external perturbations such as uniaxial[15] and hydrostatic[16,17] pressure and electric fields.[18–20] Since in amorphous matrices spectral holes are narrower than the corresponding inhomogeneous bands by 3–4 orders of magnitude, small pressure changes of a few hPa and small electric-field strengths of a few kV/cm are sufficient to give rise to easily and accurately measurable effects. External fields of these magnitudes are only small perturbations, so that the matrices can be studied under near-

equilibrium conditions. Correspondingly, only the linear terms in the pertinent perturbation series need to be taken into account.[21]

The effect of hydrostatic pressure on spectral holes in polymeric samples was found to consist in a shift and a concomitant broadening. In all materials studied so far, the shift occurred towards lower (higher) frequencies upon pressure increase (decrease), whereas the widths of the holes increased for all amorphous samples under investigation, irrespective of the sign of the pressure change. From the pressure-induced hole shifts it was possible to determine macroscopic thermodynamic-mechanical properties of the host matrices, such as their compressibilities by means of a purely optical experiment.[22] For the evaluation of the data a simple phenomenological model was used.

In a recent paper,[23] Laird and Skinner proposed a microscopic theory of the effects of hydrostatic pressure on hole-burning spectra. Based on very fundamental ideas about the origin of inhomogeneous broadening, it corroborates all the salient experimental findings of the pressure-tuning experiments.[16,22] With the same theoretical approach, the authors could also shed light on the internal structure of an inhomogeneous absorption band and explain its properties in terms of microscopic parameters of the molecular potentials involved.[9]

In the present paper, we extend Laird and Skinner's calculation which, in its original form, takes only the dispersion interaction into account, to include the electrostatic polarization of the dye molecules by the matrix field. This additional interaction leads to the induction of static electric-dipole moments in centrosymmetric absorbers and manifests itself in the occurrence of a linear Stark effect of spectral holes.[18–20] In a way analogous to Ref. 23 we obtain a distribution function for the induced dipole-moment difference μ (in order to simplify our notation, especially in the theory section, we do not use the symbol "Δ" for denoting difference quantities) between the excited and the ground state of the guest molecules and a variation of its most probable value with the frequency within the inhomogeneous band.

In Sec. II we report on Stark-effect measurements of persistent spectral holes burned in the system octaethylporphin in poly(styrene). Indeed we observed a variation of the average matrix-induced μ value across the inhomogeneous line, namely an increase from higher to lower frequencies. The comparison of the magnitude of this variation with the theoretical calculations leads to the unequivocal conclusion that the solvent shift in our system is largely determined by the van der Waals interaction. The contribution of the electrostatic polarization of the dye molecules is smaller by about 2 orders of magnitude, even though this interaction mechanism alone is responsible for the induction of the permanent dipole moments that give rise to the observed linear Stark effect.

The paper is organized as follows. In Sec. II we describe our experiment and present the data. Here we show that the matrix-induced dipole-moment difference μ as well as the quasihomogeneous linewidth γ, as measured in a hole-burning experiment, increase from the blue to the red edge of the inhomogeneous band. Section III contains two theoretical approaches for connecting μ with the pertinent solvent-shift value. The first one is a very simple electrostatic model that does not take the dispersive forces into account, whereas the second one is the extension of Laird and Skinner's theory mentioned above.[23] In Sec. IV we compare the results of our calculation with the experimental μ variation and discuss the physical implications. Finally in Sec. V the conclusions are given.

II. EXPERIMENTAL

A. Technical details

Within the scope of the present study we performed Stark-effect experiments on persistent spectral holes burned in the lowest-energy optical-absorption band of octaethylporphin (OEP) that was dissolved in the amorphous polymer poly(styrene) (PS). This absorption band, which corresponds to the electronic $|S_1\rangle \leftarrow |S_0\rangle$ (0-0) transition, is centered around 16 168 cm^{-1}. The first step in the sample preparation was dissolving the dye and the polymer in chloroform. After evaporation of this solvent in a vacuum box, colored pieces of PS were obtained. They were subsequently heated to a temperature around the glass point of the host matrix (100 °C) and pressed between two glass plates that carried electrically conducting but optically transparent, *p*-type doped indium oxide layers on their inner sides. The specific resistance of the layers was about 300 Ω m. These plates served as electrodes for applying static electric fields. On both sides of the sample small pieces of a 100-μm-thick poly(ethylene terephthalate) foil were inserted between the plates for adjusting the thickness. The exact values of the thickness were finally measured with an inductive translation probe; the thickness was constant across the area of the samples within typically $\pm 5\%$. The doping concentrations were on the order of 10^{-3} mol dye per mole of the monomer, resulting in amplitudes of the lowest-energy absorption band between 0.5 and 0.7 in units of optical density.

The samples were cooled down to 1.5 K by immersing them in superfluid helium in a custom-built ^{4}He-bath cryostat. The temperature was measured with a calibrated carbon resistor. During an experimental series, which usually took 2 to 3 h, the temperature was kept constant within ± 0.02 K by controlling the vapor pressure of the helium. The holes were burned and detected with an actively stabilized tunable single-mode cw dye laser Coherent 599-21, which provided linearly polarized light with a bandwidth of about 1×10^{-4} cm^{-1}. The hole spectra were obtained by recording the normalized transmission signal of the sample (see Fig. 1). In order to achieve a good signal-to-noise ratio, a lock-in technique was used for detection.

B. Results

The measurements were performed in the following way. A hole was burned with a certain external field strength applied (in most cases zero) and first recorded

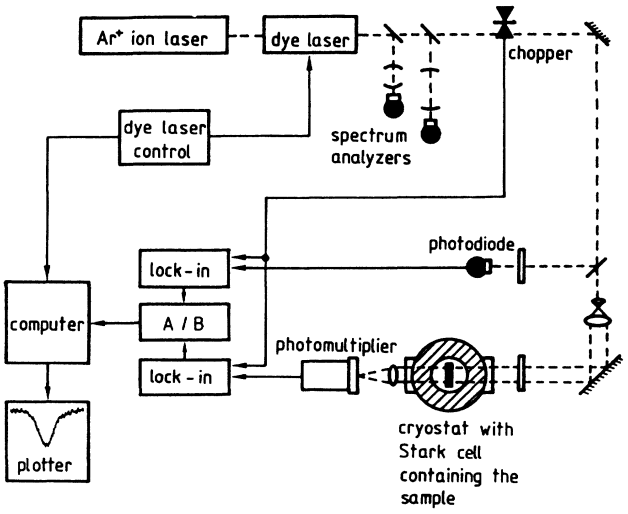

FIG. 1. Experimental setup used for burning and detecting persistent spectral holes.

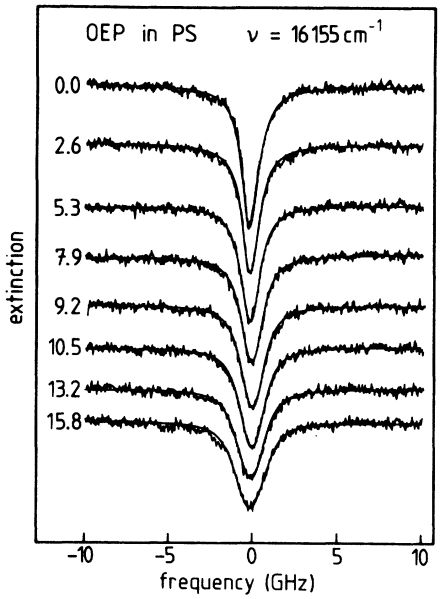

FIG. 2. Stark effect of a persistent spectral hole in OEP/PS. The numbers in the plot denote the applied electric-field strengths in kV/cm. The hole is located at 16 155 cm^{-1}. The fit curves correspond to $\bar{\mu}=0.0763$ D; their heights have been corrected for a backreaction of the photoproduct.

without altering this field condition. Only zero-phonon holes were investigated. Then the applied field strength was changed in several steps (usually ten) and each time the spectrum was recorded. From the applied field strengths and the corresponding hole widths the average matrix-induced dipole-moment differences of the dye molecules were calculated by using the fit procedure as outlined in Ref. 19. For the dielectric constant of PS, which enters in the Lorentz correction factor of the local-field strength in the matrix,[19] we inserted the value of $\epsilon=2.5$.[24] The evaluation method is based on a simple phenomenological model that neglects the dichroic character of a hole[25,26] and, hence, assumes that there is an isotropic angular distribution of the dipole-moment difference vectors among the molecules contributing to the hole. For the distribution function of the absolute values of these vectors we used the form

$$g(\mu)=\frac{4}{\pi^{1/2}\mu_p^3}\mu^2\exp\left[-\left[\frac{\mu}{\mu_p}\right]^2\right], \quad (1)$$

which was originally proposed by Bogner *et al.*[27]

Figure 2 shows a series of scans over a hole burned near the center of the inhomogeneous line, with different electric-field strengths applied. From the increase of its width, an average dipole-moment difference of $\bar{\mu}=(0.076\pm0.008)$ D was calculated. $\bar{\mu}$ is connected with the peak value μ_p of the distribution in Eq. (1) via $\bar{\mu}=(2/\sqrt{\pi})\mu_p$. The theoretical curves overlaid over the experimental spectra in Fig. 2 were obtained with this $\bar{\mu}$ value, however, their amplitudes were slightly adjusted to take into account a slow decrease of the hole area that occurred during the experimental series.[19] The comparison of experimental and calculated hole profiles shows that our model reflects the salient features of the hole-broadening process caused by the linear Stark effect. Furthermore, it has the advantage that the evaluation procedure of the measurements is a simple nonlinear optimization with only one fit parameter ($\bar{\mu}$). In the past years, several more elaborate theories have been published[18,28–30] that do not neglect the inherent anisotropy of spectral holes. However, the evaluation of Stark-effect experiments according to these theories is more complicated and requires much more computing time, since usually more than one parameter must be fitted. Moreover, they are strictly valid only in the limit of very shallow holes in which the bleaching of the optical anisotropy due to the photochemical saturation is negligible.[25] On the other hand, burning holes of intermediate depths (mainly between 20% and 50% of the height of the absorption band) proved to be preferable in order to achieve a favorable signal-to-noise ratio also in the case of strong Stark-effect broadening. It was tested that the results obtained with the method of Ref. 19 were independent of the initial hole depth within experimental accuracy. It was also checked that the broadening phenomena observed were fully reversible for the applied field strengths below about 100 kV/cm: when the field was turned off after the end of a series of scans, the hole width reduced to its original value.

In Fig. 3 we present the results of our measurements of $\bar{\mu}$ at different frequencies in the inhomogeneous absorption band. The increase from the blue to the red edge of the band is quite obvious. In part (a) the $\bar{\mu}$ values and in part (b) their squares have been plotted versus frequency. In both cases the straight line corresponds to a linear least-squares fit. In the linear plot it has a slope of $(-3.1\pm0.12)\times10^{-4}$ D/cm^{-1} and intersects the abscissa at 16 430±80 cm^{-1}, whereas in the plot of $(\bar{\mu})^2$ the corresponding numbers are $(-5.8\pm1.1)\times10^{-5}$ D^2/cm^{-1} and 16 280±90 cm^{-1}. Due to the scatter of the data points, we cannot decide in which case the linear fit is better. According to our theoretical models, however, the quad-

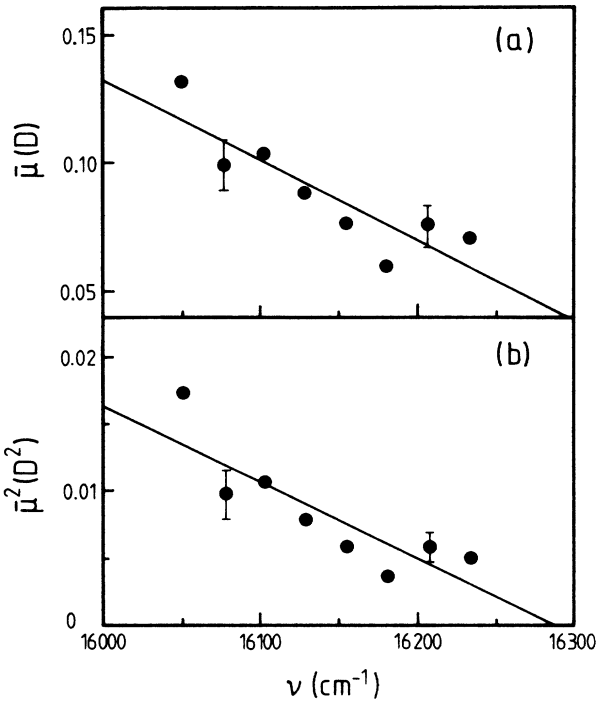

FIG. 3. Average induced dipole-moment differences $\bar{\mu}$ measured at various positions in the inhomogeneous absorption band. In part (a) the $\bar{\mu}$ values and in part (b) their squares have been plotted vs frequency. In each case the straight line was obtained by a least-squares fit.

ratic plot seems to be more appropriate for a physical interpretation (see Secs. III and IV).

We already reported a variation of the matrix-induced $\bar{\mu}$ values with the position in the lowest-energy optical-absorption bands for two other dye-polymer systems, namely a symmetrically substituted Zn-tetrabenzoporphin in poly(vinyl butyral) and pentacene in poly(methyl methacrylate)[21] (PMMA). This effect therefore seems to occur in a wide variety of systems with host materials both polar and apolar.

The phenomenon that centrosymmetric dye molecules embedded in an apolar matrix such as PS exhibit a linear Stark effect is surprising; however, it was recently also reported for solid solutions of perylene in poly(ethylene), *n*-octodecane, and solid paraffin oil.[20] The authors of Ref. 20 ascribed it to slight electric-field-induced changes of the dispersion interaction between a dye molecule and its surroundings. In the case of the PS matrix, on the other hand, it may really be due to permanent electric matrix fields, because the phenyl rings of the styrene units are asymmetrically substituted with respect to the polymer backbone and, thus, carry small electric-dipole moments. The magnitude of these moments should be similar to the value of toluene, which, in the gas phase, was measured as 0.36±0.05 D (Ref. 31). In Sec. IV we will show that a dipole moment of this size of the styrene units is consistent with our data presented in Fig. 3.

We also measured the quasihomogeneous linewidth γ of our hole-burning system at various positions within the inhomogeneous absorption band. In order to obtain this quantity at a given frequency, we burned a series of six or seven holes close to one another with decreasing burning fluences. They covered a frequency region of typically 2.3 cm^{-1}, which is only a small fraction of the inhomogeneous bandwidth of 152 cm^{-1}. The quasihomogeneous linewidth was calculated by linear extrapolation of their half-widths [half-width at half maximum (HWHM)] to zero-burning fluence.[32] We call this width quasi homogeneous, since it may contain contributions of spectral-diffusion processes that take place on time scales shorter than the duration of the experiment of a few minutes.[33–35] Figure 4 shows that there is a distinct variation of the linewidths with burning frequency. The increase from the blue to the red edge of the band is analogous to the case of the $\bar{\mu}$ values. The linear-regression line in Fig. 4 has a slope of 1.78±0.15 MHz/cm^{-1} and it reaches the T_1 limit of 10.8 MHz (Refs. 36 and 37) at a photon energy of 16 610±90 cm^{-1}. The comparison between Figs. 3 and 4 suggests that there must be some correlation between the electrostatic dye-matrix interaction that causes the induction of the dipole moments, and the dynamical processes that give rise to dephasing and spectral diffusion and, in this way, determine the optical linewidth.

A dependence of the widths of photochemical holes on burning frequency was already reported for the system OEP in PS.[36,37] The authors performed hole-burning experiments between 0.05 and 1.5 K at two wavelengths in the lowest-energy absorption band, namely at 620.1 and 621.8 nm. At 1.5 K, they measured hole widths of 900±50 and 1070±50 MHz, respectively. The corresponding linewidth values (half the hole widths) are located slightly above the linear-regression line calculated from our measurements (see Fig. 4), probably because the data were not obtained by extrapolation to zero-burning fluence. Nevertheless, they show the same trend that holes are broader at longer wavelengths. At the very low temperature of 50 mK, the variation seems to be even more pronounced; in this case hole widths of 26±1.5 and

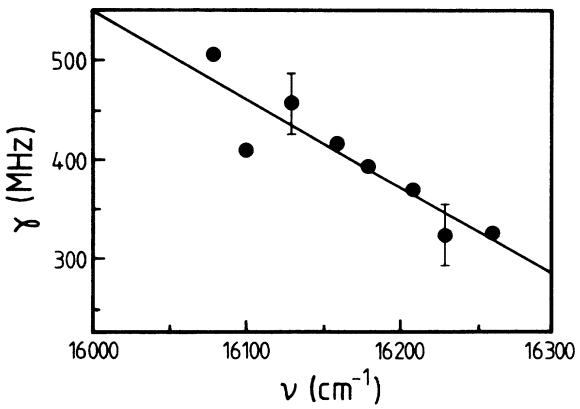

FIG. 4. Optical zero-phonon linewidths measured at various positions in the inhomogeneous absorption band. Each data point was obtained by extrapolation of the half-widths of a series of holes to zero-burning fluence. The straight line corresponds to a least-squares fit.

34±1.5 MHz, respectively, were measured at the two wavelengths.[36,37]

III. THEORY

A. Line shift and induced dipole-moment difference of centrosymmetric dye molecules due to the electric matrix field

Let us consider an apolar dye molecule as an impurity in an amorphous solid, for instance a polymer. At its position it experiences the local internal matrix field strength $\mathbf{E}_{\text{int}}$. We can assume that $\mathbf{E}_{\text{int}}$ has a random orientation with respect to the molecular coordinate system. Furthermore, we also use the simplification that the polarizability of the molecule changes isotropically upon electronic excitation so that the difference between the two polarizability tensors can be described by the unit tensor, multiplied by a scalar, α. In this case the induced dipole-moment difference is simply

$$\boldsymbol{\mu}=\alpha\mathbf{E}_{\text{int}} . \tag{2}$$

Since the energy shift of each of the two electronic states is given by the interaction between the induced dipole moment and the matrix field, the absorption line shifts by the value

$$\nu_s'=-\frac{1}{2hc}\alpha E_{\text{int}}^2 , \tag{3}$$

(in wave-number units) with h being Planck's constant and c the velocity of light. We do not consider the effect of the external electric field applied in a Stark-effect experiment, because it is much weaker than E_{int}; otherwise, not only the linear but also the quadratic Stark effect would play a role in the broadening of the holes. Equation (2) can be inserted into Eq. (3) so that the internal field strength is eliminated:

$$\mu^2=-2hc\alpha\nu_s' . \tag{4}$$

ν_s' is the line shift of the dye molecule due to the purely electrostatic polarization in the matrix field; it does not contain the contribution of the dispersion interaction. It should be noted that Eq. (4) holds also in the case of a disklike change of the molecular polarizability, i.e., when two diagonal elements of the difference tensor are equal to α and all other elements are zero. If ν_s' described the total solvent shift, the square of the matrix-induced dipole-moment difference of a centrosymmetric dye molecule should vary across the absorption band in a linear fashion. In this case, the straight line as given by Eq. (4) would extrapolate to the vacuum absorption frequency for $\mu=0$, and its slope would yield the α value.

In order to obtain an estimate, whether or not it is a good approximation to neglect the influence of the dispersion interaction, we evaluate our experimental data in terms of Eq. (4). From the slope of the linear-regression line in Fig. 3(b), a polarizability difference between the excited and the ground state of

$$\frac{\alpha}{4\pi\epsilon_0}=0.15\pm0.03\ \text{Å}^3$$

is calculated for OEP, with ϵ_0 being the permittivity of vacuum (in SI units). This value is very small compared to typical data of other molecules having a similar size. The principal α values were determined for tetracene and pentacene from the second-order Stark effect caused by an external electric field, when the molecules were embedded in p-terphenyl single crystals at 1.5 K.[38] The values of 65, 23, and -8 Å^3 were obtained for tetracene and 131, 76, and -32 Å^3 for pentacene, respectively, with error margins ranging between ±3 Å^3 and ±10 Å^3.[39] Corresponding literature data were not found for porphyrin dyes, but the polarizability differences should be of comparable magnitude in this class of molecules. Therefore, the α value obtained by evaluating our data in terms of the simple electrostatic model is too small by about 2–3 orders of magnitude.

The above model of viewing the large organic dye molecules as polarizable point dipoles is certainly a very crude approximation. Because of the spatial extent of their π electron system, higher-order multipole moments will—especially in the excited state—make non-negligible contributions to the charge distribution of the molecules in the electric matrix field. However, it seems unlikely that these higher-order moments can give rise to an error in the determination of α by 2–3 orders of magnitude. The measurements of the quadratic Stark effect of tetracene and pentacene in p-terphenyl could also be explained by taking only the first-order polarizabilities into consideration.[38,39] Thus we must conclude that the simple electrostatic model is fundamentally incorrect.

B. Microscopic theory of the correlation between solvent shift and matrix-induced dipole moments

In the preceding section we saw that our experimental data cannot be satisfactorily explained without taking into account the contribution of the dispersion interaction (van der Waals interaction) to the solvent shift. In the following, we present a modification of Laird and Skinner's theory[23] that describes both the solvent shift (including the dispersive part) and the matrix-induced dipole-moment differences in a microscopic fashion and, thus, explains the correlation between these two quantities.

We start out by defining the probability distribution $P(\mathbf{R}_1,\ldots,\mathbf{R}_N)$ for solvent molecules being located at the position vectors $\mathbf{R}_1$ through $\mathbf{R}_N$, with respect to a dye molecule. If, as in our case, the host matrix is a polymer, the monomeric units can be regarded as solvent molecules. Since the perturbations of the electronic wave functions of the solute are due to a large number of randomly oriented solvent units, we make the simplifying assumption that the interaction depends only on their positions but not on their orientations. The probability function is normalized in the following way:

$$\int d\mathbf{R}_1\cdots\int d\mathbf{R}_N\,P(\mathbf{R}_1,\ldots,\mathbf{R}_N)=V^N , \tag{5}$$

with V being the volume of the sample. Having defined the function $P(\mathbf{R}_1,\ldots,\mathbf{R}_N)$ we can immediately write down an expression for the inhomogeneous distribution of absorption lines of the dye molecules in the sample,[23]

$$I(\nu)=V^{-N}\int d\mathbf{R}_1\cdots\int d\mathbf{R}_N\,P(\mathbf{R}_1,\ldots,\mathbf{R}_N)\times\delta\left[\nu-\sum_{m=1}^{N}\tilde{\nu}(\mathbf{R}_m)\right]. \quad (6)$$

Here, $\tilde{\nu}(\mathbf{R}_m)$ is the line shift of a solute due to the interaction with a solvent unit that is located at the position $\mathbf{R}_m$. Note that the inhomogeneous absorption band, as observed in a spectrometer, is the convolution of $I(\nu)$ with the homogeneous absorption line.

In order to find a correlation between the squared matrix-induced dipole-moment difference μ^2 and the solvent shift ν, we calculate the conditional probability $f(\mu^2|\nu)$ of a molecule having the value of μ^2 if its solvent shift is ν. For mathematical reasons, which will become clear later on, we consider μ^2 rather than μ. Furthermore, in this way our results can be more readily compared with those of the simple electrostatic model presented above. An expression for $f(\mu^2|\nu)$ is obtained in a similar way as for $I(\nu)$:

$$f(\mu^2|\nu)=[I(\nu)V^N]^{-1}\int d\mathbf{R}_1\cdots\int d\mathbf{R}_N\,P(\mathbf{R}_1,\ldots,\mathbf{R}_N)\times\delta\left[\nu-\sum_{m=1}^{N}\tilde{\nu}(\mathbf{R}_m)\right]\times\delta\left[\mu^2-\sum_{m=1}^{N}\zeta(\mathbf{R}_m)\right]. \quad (7)$$

$\zeta(\mathbf{R}_m)$ defines the square of the dipole-moment difference that is induced in a dye molecule by the mth solvent unit. Mathematical expressions for $\tilde{\nu}(\mathbf{R}_m)$ and $\zeta(\mathbf{R}_m)$ will be specified later on. At first, however, we must introduce an approximation to make the integrals in Eqs. (6) and (7) tractable. We assume that the positions of the solvent molecules are statistically independent of each other so that $P(\mathbf{R}_1,\ldots,\mathbf{R}_N)$ can be factorized into a product of N equal two-particle solute-solvent distribution functions,

$$P(\mathbf{R}_1,\ldots,\mathbf{R}_N)=\prod_{m=1}^{N}g(\mathbf{R}_m). \quad (8)$$

This approximation restricts the applicability of our calculation to amorphous systems. The next step is to express the δ functions by their Fourier representations. Following the mathematical procedure of Ref. 23, we arrive at the result

$$I(\nu)=(2\pi)^{-1}\int_{-\infty}^{+\infty}dx\,e^{i\nu x}e^{-\rho J(x)}, \quad (9)$$

$$f(\mu^2|\nu)=[4\pi^2 I(\nu)]^{-1}\int_{-\infty}^{+\infty}dx\int_{-\infty}^{+\infty}dy\,e^{i\nu x}e^{i\mu^2 y}\times e^{-\rho j(x,y)}, \quad (10)$$

with

$$J(x)=\int d\mathbf{R}\,g(\mathbf{R})(1-e^{-i\tilde{\nu}(\mathbf{R})x}), \quad (11)$$

$$j(x,y)=\int d\mathbf{R}\,g(\mathbf{R})(1-e^{-i\tilde{\nu}(\mathbf{R})x}e^{-i\zeta(\mathbf{R})y}). \quad (12)$$

In these equations, $\rho=N/V$ is the number density of the solvent molecules in the bulk of the sample.

The distribution functions $I(\nu)$ and $f(\mu^2|\nu)$ have been expressed as the Fourier transforms of the exponentials of $J(x)$ and $j(x,y)$, respectively. These two new functions contain all the information about the interaction between a dye molecule and its matrix environment. For physically meaningful forms of $\tilde{\nu}(\mathbf{R})$ and $\zeta(\mathbf{R})$, their spatial integrations can usually not be carried out in an analytical fashion. However, there is a way to obtain a reasonable approximation, as can be seen from their functional dependences. For x and y close to zero, large values of the interaction potentials $\tilde{\nu}(\mathbf{R})$ and $\zeta(\mathbf{R})$, which are physically most important, still yield sizeable contributions to $J(x)$ and $j(x,y)$. Therefore, we can expand these functions into Taylor series up to the second-order terms. This is called the Gaussian approximation.[23] The result is

$$J(x)\cong iAx+\tfrac{1}{2}Bx^2, \quad (13)$$

$$j(x,y)\cong iAx+iCy+\tfrac{1}{2}Bx^2+\tfrac{1}{2}Dy^2+Exy \quad (14)$$

with

$$A=\int d\mathbf{R}\,g(\mathbf{R})\tilde{\nu}(\mathbf{R}), \quad (15a)$$

$$B=\int d\mathbf{R}\,g(\mathbf{R})[\tilde{\nu}(\mathbf{R})]^2, \quad (15b)$$

$$C=\int d\mathbf{R}\,g(\mathbf{R})\zeta(\mathbf{R}), \quad (15c)$$

$$D=\int d\mathbf{R}\,g(\mathbf{R})[\zeta(\mathbf{R})]^2, \quad (15d)$$

$$E=\int d\mathbf{R}\,g(\mathbf{R})\tilde{\nu}(\mathbf{R})\zeta(\mathbf{R}). \quad (15e)$$

After inserting Eqs. (13) and (14) into Eqs. (9) and (10), the Fourier integrals can be solved, yielding

$$I(\nu)=(2\pi\sigma_s^2)^{-1/2}\exp\left[-\frac{(\nu-\nu_s)^2}{2\sigma_s^2}\right],$$
$$\nu_s=\rho A, \quad (16)$$
$$\sigma_s=(\rho B)^{1/2},$$
$$f(\mu^2|\nu)=(2\pi\sigma_\mu^2)^{-1/2}\exp\left[-\frac{(\mu^2-\mu_{\max}^2)^2}{2\sigma_\mu^2}\right],$$

$$\mu_{\max}^2=\rho\left[C+\frac{E(\nu-\nu_s)}{\sigma_s^2}\right], \quad (17)$$

$$\sigma_\mu=\left[\rho\left[D-\frac{\rho E^2}{\sigma_s^2}\right]\right]^{1/2}.$$

According to these results, both the inhomogeneous band shape $I(\nu)$ and the distribution of μ^2 values at a specific frequency are described by normalized Gaussian profiles [hence the name *"Gaussian approximation"* of the Taylor expansions in Eqs. (13) and (14)]. The maximum value $\mu^2_{\max}$ of the μ^2 distribution depends on frequency in a linear fashion and, thus, varies with the position within the inhomogeneous band. This is in agreement with our experimental findings [see Fig. 3(b)]. A similar behavior was also calculated for the pressure shift coefficient of persistent spectral holes.[23] We wish to emphasize again that also a linear plot of the $\bar{\mu}$ values, which have even smaller relative errors, can be well fitted with a straight line [Fig. 3(a)]. However, according to our theory, the quadratic plot seems to us more appropriate for a physical interpretation of the data within the Gaussian approximation.

A variation of the matrix-induced dipole-moment difference across the inhomogeneous line was already described by the simple electrostatic model presented above. According to that model, however, a certain solvent shift ν'_s was unequivocally correlated with one certain μ^2 value [see Eq. (4)]. In order to account for our experimental hole spectra, on the other hand, we had to assume that there is a distribution of dipole-moment differences amongst the molecules contributing to the hole. The microscopic theory automatically yields this result. Physically, the presence of a distribution of dipole-moment differences at a certain position in the band is a consequence of the fact that there are two mechanisms contributing to the solvent shift, namely the electrostatic polarization and the dispersion interaction, whereas only the electrostatic interaction gives rise to the induction of dipole moments. Thus the relative contributions of the two mechanisms to the line shift can vary while their sum is constant.

The interaction potentials $\tilde{\nu}(\mathbf{R})$ and $\zeta(\mathbf{R})$ can therefore be specified in the following way:

$$\tilde{\nu}(\mathbf{R})=\frac{1}{hc}[V_{\text{disp}}(\mathbf{R})+V_{\text{el}}(\mathbf{R})] \ . \tag{18}$$

For the dispersion part, we use the modified Lennard-Jones potential of Laird and Skinner,[23]

$$V_{\text{disp}}(\mathbf{R})=\begin{cases} 4\epsilon\left[\left[\dfrac{\sigma}{R-R_0}\right]^{12}-\left[\dfrac{\sigma}{R-R_0}\right]^{6}\right] & \text{if } R\geq R_0 \\ \infty \quad \text{if } R<R_0 \ . \end{cases} \tag{19}$$

The shift in radial direction by the amount R_0 is necessary for a correct physical description if there is a large disparity in size between the dye and the matrix molecules. In this case, σ is (as in the regular Lennard-Jones form) the solvent diameter, while $R_0+\sigma/2$ can be interpreted as the solute radius. ϵ is the difference between the dispersive solute-solvent potentials in the excited and in the ground state, which are assumed to be characterized by the same R_0 value.

In order to calculate the electrostatic interaction potential $V_{\text{el}}(\mathbf{R})$, we start out with Eq. (3) and insert for the internal matrix field strength $\mathbf{E}_{\text{int}}$ the vector sum of the dipole fields of all the surrounding solvent molecules,

$$V_{\text{el}}^{\text{tot}}=hc\nu'_s=-\tfrac{1}{2}\alpha\left[\frac{1}{4\pi\epsilon_0}\right]^2\sum_{m,n}[\boldsymbol{\mu}_{1m}-3(\boldsymbol{\mu}_{1m}\cdot\hat{\mathbf{r}}_m)\hat{\mathbf{r}}_m]\cdot[\boldsymbol{\mu}_{1n}-3(\boldsymbol{\mu}_{1n}\cdot\hat{\mathbf{r}}_n)\hat{\mathbf{r}}_n]/(R_mR_n)^3 \ . \tag{20}$$

Note that $V_{\text{el}}^{\text{tot}}$ is the total electrostatic energy shift that contains the contributions of all the solvent units in the sample. Correspondingly, the m and n summations must be performed over all solvent molecules. $\boldsymbol{\mu}_{1m}$ denotes the static electric ground-state dipole moment of the mth solvent unit and $\hat{\mathbf{r}}_m$ is defined by

$$\hat{\mathbf{r}}_m=\mathbf{R}_m/R_m \ . \tag{21}$$

For the sake of simplicity the radial shift by R_0 has been temporarily omitted in Eq. (20). It will be reintroduced later on. Since we are considering identical matrix molecules, we have

$$|\boldsymbol{\mu}_{1m}|=\mu_1 \tag{22}$$

for molecules.

From our assumption of a random orientation of the solvent units it follows that the off-diagonal terms of the summations in Eq. (20) (i.e., with $m\neq n$) cancel out and only the diagonal terms survive,

$$V_{\text{el}}^{\text{tot}}=-\tfrac{1}{2}\alpha\left[\frac{1}{4\pi\epsilon_0}\right]^2\sum_m[(\boldsymbol{\mu}_{1m})^2+3(\boldsymbol{\mu}_{1m}\cdot\hat{\mathbf{r}}_m)^2]/(R_m)^6 \ . \tag{23}$$

Using the randomness of the orientation once again, we obtain for the average value of the square of the dot product

$$\langle(\boldsymbol{\mu}_{1m}\cdot\hat{\mathbf{r}}_m)^2\rangle=\tfrac{1}{3}\mu_1^2 \ , \tag{24}$$

so that Eq. (23) simplifies to

$$V_{\text{el}}^{\text{tot}}=-\alpha\left[\frac{1}{4\pi\epsilon_0}\right]^2\mu_1^2\sum_m(R_m)^{-6} \ . \tag{25}$$

Thus, it turns out that the electrostatic energy shift consists of additive contributions of the various matrix mole-

cules, the average shift due to one solvent unit being given by

$$V_{\mathrm{el}}(\mathbf{R})=-\alpha\left[\frac{1}{4\pi\epsilon_0}\right]^2\mu_1^2(R-R_0)^{-6}\ . \tag{26}$$

Here we have included the radial shift by R_0 again, which takes account of the large disparity in size between the dye and the matrix molecules. Using the abbreviation

$$\lambda=\left[\frac{1}{4\pi\epsilon_0}\right]^2\alpha\mu_1^2\sigma^{-6}\ , \tag{27}$$

we can write Eq. (26) in the concise form

$$V_{\mathrm{el}}(\mathbf{R})=-\lambda\left[\frac{\sigma}{R-R_0}\right]^6\ . \tag{28}$$

Note, that $V_{\mathrm{el}}(\mathbf{R})$ depends only on the position, not on the orientation of the matrix molecule, and can thus immediately be inserted in Eq. (18). The fact that there is a nonzero electrostatic contribution to the solvent shift, although the solvent units are oriented randomly, is analogous to the random-walk problem, in which the average distance from the starting point increases monotonically with the number of steps, while the random walker can move in all directions with equal probability.

In an analogous way as the energy shift $V_{\mathrm{el}}(\mathbf{R})$, we can also calculate the function $\zeta(\mathbf{R})$ that describes the square of the induced dipole-moment difference. The result is

$$\zeta(\mathbf{R})=2\alpha\lambda\left[\frac{\sigma}{R-R_0}\right]^6\ . \tag{29}$$

At this point it becomes clear why we have defined $f(\mu^2|\nu)$ to describe the conditional probability of finding μ^2 (rather than μ) at a given solvent shift ν [see Eq. (7)]. The Laird-Skinner formalism assumes the quantity under consideration to be composed of additive contributions of the various solvent units. As was shown in the above derivation, this is the case only for the square of the internal matrix field strength E_{int} (and, hence, the square of μ), not for E_{int} itself. Therefore, in the case of amorphous samples, the theory can be applied only to μ^2 in a straightforward manner.

The last function that must be specified to complete the theoretical model is the two-molecule solute-solvent distribution $g(\mathbf{R})$. We use the simple step function that was suggested by Laird and Skinner:[23]

$$g(\mathbf{R})=\begin{cases}1 & \text{if } R\geq R_c+R_0\\ 0 & \text{if } R<R_c+R_0\ .\end{cases} \tag{30}$$

The cutoff parameter R_c is close to the diameter σ of a solvent unit.

IV. COMPARISON WITH EXPERIMENT AND DISCUSSION

Having specified the mathematical forms of the interaction potentials $\tilde{\nu}(\mathbf{R})$ and $\zeta(\mathbf{R})$ and of the spatial distribution function $g(\mathbf{R})$, we can calculate the moments as given in Eqs. (15a)–(15e) and obtain quantitative theoretical results for the variation of μ^2 across the inhomogenous band. The moments contain integrals of the form

$$\int_{R_0+R_c}^{\infty}R^2\left[\frac{\sigma}{R-R_0}\right]^n dR=R_c^3\left[\frac{\sigma}{R_c}\right]^n\left[\frac{1}{n-3}+\frac{2}{n-2}\frac{R_0}{R_c}+\frac{1}{n-1}\left[\frac{R_0}{R_c}\right]^2\right],\quad n\geq 6 \tag{31}$$

and can thus be calculated analytically. Nevertheless, we do not give the results in full generality, since they are somewhat lengthy. Instead, we immediately insert the parameters for PS that were published in Ref. 23. They are $R_0/\sigma=0.7\pm0.1$ and $R_c/\sigma=1.045\pm0.012$. These parameters were calculated for the dye molecule free-base phthalocyanine in a PS matrix, but the size of the OEP molecule is comparable to that of phthalocyanine so that also the parameters should be very similar. The results for the moments are

$$A=-\frac{4\pi R_c^3}{hc}(1.6540\epsilon+0.5821\lambda)\ , \tag{32a}$$

$$B=\frac{4\pi R_c^3}{(hc)^2}(0.8477\epsilon^2+0.7081\epsilon\lambda+0.1686\lambda^2)\ , \tag{32b}$$

$$C=4\pi R_c^3\times2\alpha\lambda\times0.5821\ , \tag{32c}$$

$$D=4\pi R_c^3\times(2\alpha\lambda)^2\times0.1686\ , \tag{32d}$$

$$E=-\frac{4\pi R_c^3}{hc}\times2\alpha\lambda(0.3541\epsilon+0.1686\lambda)\ . \tag{32e}$$

Now we can calculate the slope of the linear variation of the squared average μ value ($\mu_{\max}^2$) with frequency. According to Eqs. (16) and (17) it is given by

$$\frac{d(\mu_{\max}^2)}{d\nu}=\frac{E}{B}=-2hc\,\alpha\lambda\frac{0.3541\epsilon+0.1686\lambda}{0.8477\epsilon^2+0.7081\epsilon\lambda+0.1686\lambda^2}\ . \tag{33}$$

First, we note that the matrix-induced dipole-moment differences increase for decreasing frequencies, provided that the solvent shift ρA is negative, which corresponds to positive values of ϵ, λ, and α. An increase of μ (or μ^2) from the blue to the red edge of the absorption band is in agreement with our experimental results (see Fig. 3). We

did not find independently measured data of the vacuum absorption frequency of OEP in the literature so that we cannot determine the sign of the solvent shift. However, the similar molecule zinc octaethylporphin has a negative solvent shift of about $-250\ \mathrm{cm}^{-1}$ in a PS matrix.[40,41]

Next we address the question of the magnitude of the slope $d(\mu^2_{\max})/d\nu$. As can be seen from Eq. (33), it is determined by the parameters ϵ and λ. If the electrostatic contribution to the solvent shift is much larger than the dispersive part ($\epsilon \ll \lambda$), we get

$$\frac{d(\mu^2_{\max})}{d\nu} = -2hc\alpha \ . \tag{34}$$

This is the same result that we already obtained with the simple electrostatic-interaction model presented in Sec. III A [Eq. (4)]. Since the α value calculated from our experimental data [Fig. 3(b)] according to Eq. (4) or (34) was unreasonably small, we concluded that this model is qualitatively incorrect. Therefore, we examine the opposite case of the dispersion interaction being the dominant part ($\epsilon \gg \lambda$). This simplifies Eq. (33) to

$$\frac{d(\mu^2_{\max})}{d\nu} = -2hc\alpha \times 0.4177 \frac{\lambda}{\epsilon} \ . \tag{35}$$

In contrast to the above case, the slope is now reduced by a factor describing the relative contributions of the electrostatic polarization and the dispersive forces to the solvent shift. Since we found the experimental slope to be smaller by 2–3 orders of magnitude than what would be expected from the simple electrostatic model, we have to conclude that the dispersion interaction yields a contribution to the solvent shift that is larger than the electrostatic-polarization part by 2–3 orders of magnitude. In a sense, this "stretches" the frequency axis by the same factor and thus causes the reduction of the slope of $\mu^2_{\max}$ versus ν. Note that the dispersion interaction is not involved in the induction of static dipole moments.

Having recognized the importance of the dispersive forces, we can test if our microscopic theory yields a reasonable value for the polarizability difference α. We insert the expression for λ [Eq. (27)] and cast Eq. (35) in the form

$$\frac{\alpha}{4\pi\epsilon_0} = 1.0941 \frac{\sigma^3}{\mu_1} \left[\left[-\frac{d(\mu^2_{\max})}{d\nu} \right] \frac{\epsilon}{hc} \right]^{1/2} \ . \tag{36}$$

For $d(\mu^2_{\max})/d\nu$ we use our experimental result $(-5.8\pm1.1)\times10^{-5}\ \mathrm{D}^2/\mathrm{cm}^{-1}$ (see Sec. II). The data $\sigma = 5.27$ Å and $\epsilon/hc = 36\pm4\ \mathrm{cm}^{-1}$ are taken from Ref. 23. Finally, for μ_1 we insert the gas-phase value of toluene $(0.36\pm0.05\ \mathrm{D})$.[31] This yields

$$\frac{\alpha}{4\pi\epsilon_0} = 20\pm4\ \text{Å}^3 \ .$$

The above result is of a reasonable order of magnitude. It is comparable to the polarizability differences measured for tetracene along the three molecular main axes.[39] From this finding we can conclude that the microscopic theory describes the dye-matrix interaction in a way that is not only qualitatively correct but yields also quantitatively satisfying predictions. Using the above result for α and our experimental $\bar{\mu}$ values [see Fig. 3(a)], we can calculate the internal electric matrix field strength E_{int}, that is experienced by the dye molecules, to vary between 9.0×10^5 and 1.9×10^6 V/cm with higher values corresponding to longer wavelengths in the inhomogeneous absorption band. These numbers are lower by approximately 1 order of magnitude than a previous estimate of the matrix field strength in polar media.[29]

Another interesting quantity that can be physically interpreted with our theory is the frequency ν_0 at which the average dipole-moment difference would reach zero. In order to deal with dimensionless numbers, we divide it by the average solvent shift ν_s. From Eqs. (16) and (17) this quotient is calculated to be

$$\frac{\nu_0}{\nu_s} = 1 - \frac{BC}{AE} \ . \tag{37}$$

Inserting the moments from Eqs. (32a)–(32e) yields

$$\frac{\nu_0}{\nu_s} = 1 - \frac{0.5821(0.8477\epsilon^2 + 0.7081\epsilon\lambda + 0.1686\lambda^2)}{(1.6540\epsilon + 0.5821\lambda)(0.3541\epsilon + 0.1686\lambda)} \ . \tag{38}$$

If the dye-matrix interaction is purely electrostatic (i.e., $\epsilon \ll \lambda$), we obtain $\nu_0 = 0$, which means that the straight regression line $\mu^2_{\max}$ versus ν intersects the frequency axis at the vacuum absorption frequency. This result is independent of the special molecular parameters R_0, R_c, and σ and is equal to that of the simple electrostatic model [see Eq. (4)]. In the opposite limit that the dispersion interaction dominates ($\epsilon \gg \lambda$), Eq. (38) yields $\nu_0 = 0.1575\nu_s$, i.e., the regression line intersects the frequency axis between the maximum of the inhomogeneous band and the vacuum absorption frequency, the distance

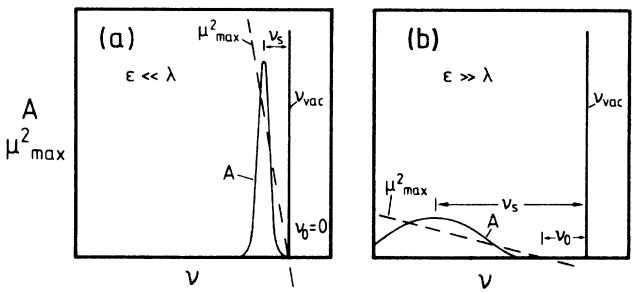

FIG. 5. Schematic showing the position and width of the inhomogeneous absorption band (A, solid line) and the variation of the mean-squared dipole-moment difference ($\mu^2_{\max}$, dashed line) with frequency in the two cases of (a) purely electrostatic dye-matrix interaction and (b) prevailing dispersion interaction. The parameters ϵ and λ are assumed to be positive. ν_s denotes the average solvent shift and ν_0 the distance of the zero point of $\mu^2_{\max}$ from the vacuum absorption frequency ν_{vac}. Note that the difference between the cases (a) and (b) is much more pronounced in reality.

from the latter being about 16% of the total difference. This number depends on the parameters R_0, R_c, and σ. The situations in the two limiting cases have been sketched schematically in Fig. 5. Note that also the position and width of the inhomogeneous absorption band are grossly different. Unfortunately, no independent measurements of the vacuum absorption frequency of OEP were reported in the literature to date.

The last quantity that we calculate with our theory is the width of the μ^2 distribution as given by Eqs. (16) and (17). With the moments obtained for the system OEP in PS [Eqs. (28)] it becomes

$$\sigma_\mu = 2\alpha\lambda \left[4\pi\rho R_c^3 \left[0.1686 - \frac{(0.3541\epsilon + 0.1686\lambda)^2}{0.8477\epsilon^2 + 0.7081\epsilon\lambda + 0.1686\lambda^2} \right] \right]^{1/2} . \tag{39}$$

Again we consider the two limiting cases of either of the interaction mechanisms being strongly dominant. For $\epsilon \ll \lambda$, Eq. (39) has the significant result $\sigma_\mu = 0$. If there are no dispersive forces in the dye-matrix system, the distribution of matrix-induced dipole-moment differences reduces to a δ function; at each frequency in the inhomogeneous line there is only one certain μ value. This is the same result that we had already obtained with the simple electrostatic model presented in Sec. III A. Thus, the microscopic theory goes over to the electrostatic model, if the van der Waals interaction is not present. The experimental finding that there is a μ (or μ^2) distribution of nonzero width, on the other hand, is now one more piece of evidence that the dispersion interaction cannot be neglected.

In the case $\epsilon \gg \lambda$ the width σ_μ depends on the molecular parameters of the dye-matrix system. For OEP in PS, Eq. (39) yields

$$\sigma_\mu = 0.1438 \times 2\alpha\lambda (4\pi\rho R_c^3)^{1/2} .$$

Using the quantity $\rho\sigma^3 = 0.8815$ as given in Ref. 23 and the expression for the polarizability difference $\alpha/4\pi\epsilon_0$ calculated above [Eq. (36)], we finally obtain

$$\sigma_\mu = (2.6 \pm 0.6) \times 10^{-3} \text{ D}^2 .$$

At this point a comment on our procedure of data evaluation seems to be necessary. In order to calculate the average matrix-induced dipole-moment differences from our experimental hole spectra, we assumed that the μ values are distributed according to Eq. (1), which is different from the distribution function as given by the microscopic theory [Eq. (17)]. The advantage of using Eq. (1) rather than Eq. (17) is that it contains ony one fit parameter so that the data evaluation is easier and numerically more stable. Qualitatively the two functions are similar, except for the fact that Eq. (1) is slightly asymmetric and that its width and maximum value are proportional to each other, whereas Eq. (17) describes a perfectly symmetric Gaussian profile (in μ^2), whose center position and width are independent. For evaluating the data this should not make a big difference, as we can see when we compare the widths of the two functions. In the asymmetric distribution [Eq. (1)], a measure for the width is the distance between the two points of maximum slope, which is approximately equal to the average value $\bar{\mu}$ (more exactly, $0.92\bar{\mu}$). In the case of the Gaussian function, the distance between the two turning points is equal to $2\sigma_\mu$, which was obtained as

$$2\sigma_\mu = (5.1 \pm 1.1) \times 10^{-3} \text{ D}^2$$

(see above). A comparison with Fig. 3(b) shows that this result is close to the $\bar{\mu}^2$ values measured near the center of the inhomogeneous band. Although the width of the Gaussian distribution is, in principle, not correlated to the average value, the numerical relationship between these two quantities is thus similar to that of the asymmetric function.

In order to obtain an estimate for the width $\sigma_{\mu,\text{lin}}$ of the μ distribution on a linear scale, we calculate the difference between the square-root values of μ^2 at the two points of maximum slope of the function $f(\mu^2|\nu)$. Using our above result $\sigma_\mu = (2.6 \pm 0.6) \times 10^{-3}$ D^2 and a mean value of $\mu^2_{\text{max}} = 8.0 \times 10^{-3}$ D^2, we obtain

$$\sigma_{\mu,\text{lin}} = 0.029 \pm 0.007 \text{ D} .$$

This width is somewhat smaller than the measured average dipole-moment differences $\bar{\mu}$. In Fig. 3(a) we have a variation between $\bar{\mu} = 0.060$ D and $\bar{\mu} = 0.130$ D from the blue to the red edge of the absorption band. Nevertheless, we see that also on a linear scale the width of the μ distribution at a certain position in the band, as calculated from our microscopic theory, is of the same order of magnitude as the average values.

V. SUMMARY AND CONCLUSIONS

For the system octaethylporphin in poly(styrene), we have presented the results of Stark-effect experiments on persistent spectral holes burnt in the lowest-energy optical-absorption band of the dye. In an external electric field the holes exhibit a symmetrical broadening that is due to static matrix-induced dipole moments. Although poly(styrene) is a pure hydrocarbon, the phenyl side groups carry small electric-dipole moments because of their asymmetric substitution, with respect to the polymer backbone. These moments give rise to the matrix field that polarizes the dopant molecules. Measurements performed at various wavelengths within the inhomogeneous absorption band showed that the average matrix-induced dipole-moment difference $\bar{\mu}$ between the electronic excited and ground state increases from the

blue to the red edge of the band by roughly a factor of 2. The quasihomogeneous optical linewidth γ as obtained by extrapolating the hole widths to zero-burning fluence, exhibits a similar behavior. These results demonstrate that the electrostatic dye-matrix interaction that manifests itself in the induced dipole moments, and the dynamic interaction as expressed in the linewidths, are correlated with each other and with the solvent shift in the system investigated.

In order to explain the variation of $\bar{\mu}$, we first applied a simple electrostatic model, according to which the solvent shift is entirely given by the second-order Stark effect of the centrosymmetric dye molecules in the matrix field. While the increase of $\bar{\mu}$ from the blue to the red edge of the band is described in a qualitatively correct way, its magnitude is off by about 2 orders of magnitude. Moreover, the model does not account for the experimental finding that at each wavelength there is a distribution of dipole-moment differences around $\bar{\mu}$ rather than one single value.

This failure of the simple model led us to conclude that the dispersion interaction yields a substantial contribution to the solvent shift and cannot be neglected. Therefore we modified a microscopic theory published recently by Laird and Skinner[23] and expanded it to our problem. In its original form it was used to describe the reversible shift and broadening of spectral holes by hydrostatic pressure. Our extended theoretical approach calculates the matrix-induced dipole-moment differences at each position in the inhomogeneous band, thereby taking the effects of both the dispersive forces and the electrostatic interaction into account. The theory predicts a linear increase of the square of $\bar{\mu}$ from higher to lower frequencies in the band. Contrary to the simple electrostatic model, however, it even yields a correct value for the magnitude of this variation, if the contribution of the dispersion interaction to the solvent shift is much larger than that of the electrostatic polarization. In addition, the present theory takes into account that there is a distribution of dipole-moment differences at each wavelength position.

The comparison between the results of the two models and a critical evaluation of our experimental data leads to the conclusion that the contribution of the dispersive forces to the solvent shift is larger than the electrostatic part by roughly 2 orders of magnitude. Physically, this means that the van der Waals interaction "enhances" the line shift due to the static second-order Stark effect by a factor of about 100 and in this way "stretches" the frequency axis as compared to the electrostatic model so that the slope of the regression line of $\bar{\mu}^2$ versus ν is reduced by the same factor. It is an interesting finding that the two interaction mechanisms, being of totally different physical origins, yield line-shift contributions, which differ by 2 orders of magnitude but are nevertheless correlated.

The microscopic theory originally developed by Laird and Skinner[23] turned out to be a very powerful tool for describing the interaction between the dye molecules and their matrix environment. The effects of hydrostatic pressure and of static electric fields on persistent-hole spectra are now understood in the framework of one common formalism, at least in the case of poly(styrene) doped with centrosymmetric porphyrin dyes. In the present paper we showed that the Stark-effect data can be explained with the same microscopic parameters that were independently obtained in Ref. 23 from the evaluation of the pressure tuning experiments. Future investigations will show if the theory can also adequately describe the situation of systems containing strongly polar matrix and/or polar dye molecules. Another direction in which the theory may give rise to deeper insight is the description of optical linewidths. We did not address this problem in the present paper. Our measuremetns show, however, that the linewidth varies across the inhomogeneous band in a way that is similar to the matrix-induced dipole moments. Therefore, a correlation between the dynamic dye-matrix interaction and the (static) solvent shift should be accounted for by future linewidth theories.

ACKNOWLEDGMENTS

This work was supported by the Stiftung Volkswagenwerk, Hannover, Germany, by the Deutsche Forschungsgemeinschaft (Sonderforschungsbereich No. SFB-213), Bonn, Germany, and by the Alexander von Humboldt Foundation (R.S.), Bonn, Germany. We also acknowledge support by the Fonds der Chemischen Industrie. Furthermore, we would like to thank our colleagues A. Blumen, J. Friedrich, W. Richter, and Th. Sesselmann at the University of Bayreuth for valuable discussions.

[1]Y. Ooshika, J. Phys. Soc. Jpn. **9**, 594 (1954).
[2]H. C. Longuet-Higgins and J. A. Pople, J. Chem. Phys. **27**, 192 (1957).
[3]E. G. McRae, J. Phys. Chem. **61**, 562 (1957).
[4]W. Liptay, Angew. Chem. **81**, 195 (1969); Angew. Chem. Int. Ed. Engl. **8**, 177 (1969), and references therein.
[5]W. E. Henke, W. Yu, H. L. Selzle, E. W. Schlag, D. Wutz, and S. H. Lin, Chem. Phys. **97**, 205 (1985).
[6]D. M. Burland and D. Haarer, IBM J. Res. Dev. **23**, 534 (1979).
[7]D. Haarer and M. R. Philpott, in *Spectroscopy and Dynamics of Condensed Matter Systems,* Vol. 4 of *Modern Problems in Condensed Matter Sciences,* edited by V. M. Agranovich and R. M. Hochstrasser (North-Holland, Amsterdam, 1983), p. 27.
[8]A. M. Stoneham, Rev. Mod. Phys. **41**, 82 (1969).
[9]B. B. Laird and J. L. Skinner, J. Chem. Phys. **90**, 3880 (1989).
[10]L. A. Rebane, A. A. Gorokhovskii, and J. V. Kikas, Appl. Phys. B **29**, 235 (1982).
[11]R. I. Personov, in *Spectroscopy and Dynamics of Condensed Matter Systems,* Vol. 4 of *Modern Problems in Condensed Matter Sciences* (Ref. 7), p. 55.
[12]G. J. Small, in *Spectroscopy and Dynamics of Condensed Matter Systems,* Vol. 4 of *Modern Problems in Condensed*

Matter Sciences (Ref. 7), p. 515.
[13]J. Friedrich and D. Haarer, Angew. Chem. **96**, 96 (1984); Angew. Chem. Int. Ed. Engl. **23**, 113 (1984).
[14]*Persistent Spectral Hole Burning: Science and Applications,* edited by W. E. Moerner (Springer, Berlin, 1988).
[15]W. Richter, G. Schulte, and D. Haarer, Opt. Commun. **51**, 412 (1984).
[16]Th. Sesselmann, W. Richter, D. Haarer, and H. Morawitz, Phys. Rev. B **36**, 7601 (1987).
[17]A. Oppenländer, J.-C. Vial, R. M. Macfarlane, and J.-P. Chaminade, J. Lumin. **42**, 331 (1989).
[18]A. J. Meixner, A. Renn, S. E. Bucher, and U. P. Wild, J. Phys. Chem. **90**, 6777 (1986).
[19]L. Kador, D. Haarer, and R. I. Personov, J. Chem. Phys. **86**, 5300 (1987).
[20]J. Gerblinger, U. Bogner, and M. Maier, Chem. Phys. Lett. **141**, 31 (1987).
[21]Th. Sesselmann, L. Kador, W. Richter, and D. Haarer, Europhys. Lett. **5**, 361 (1988).
[22]Th. Sesselmann, W. Richter, and D. Haarer, J. Lumin. **36**, 263 (1987).
[23]B. B. Laird and J. L. Skinner, J. Chem. Phys. **90**, 3274 (1989).
[24]*Polymer Handbook,* 2nd ed., edited by J. Brandrup and E. H. Immergut (Wiley, New York, 1975), p. VIII-7.
[25]W. Köhler, W. Breinl, and J. Friedrich, J. Phys. Chem. **89**, 2473 (1985).
[26]I. S. Osad'ko, S. L. Soldatov, and A. U. Jalmukhambetov, Chem. Phys. Lett. **118**, 97 (1985).
[27]U. Bogner, P. Schätz, R. Seel, and M. Maier, Chem. Phys. Lett. **102**, 267 (1983).
[28]B. M. Kharlamov and N. I. Ulitsky, Institute for Spectroscopy Report No. 12, Troitsk, Moscow, 1986 (unpublished).
[29]M. Maier, Appl. Phys. B **41**, 73 (1986).
[30]P. Schätz and M. Maier, J. Chem. Phys. **87**, 809 (1987).
[31]*CRC Handbook of Chemistry and Physics,* 61st ed., edited by R. C. Weast and M. J. Astle (CRC Press, Boca Raton, 1980), p. E-66.
[32]L. Kador, G. Schulte, and D. Haarer, J. Phys. Chem. **90**, 1264 (1986).
[33]C. A. Walsh, M. Berg, L. R. Narasimhan, and M. D. Fayer, J. Chem. Phys. **86**, 77 (1987).
[34]L. R. Narasimhan, D. W. Pack, and M. D. Fayer, Chem. Phys. Lett. **152**, 287 (1988).
[35]A. Rebane and D. Haarer, Opt. Commun. **70**, 478 (1989).
[36]A. A. Gorokhovskii, V. Kh. Korrovits, V. V. Pal'm, and M. A. Trummal, JETP Lett. **42**, 307 (1985) [Pis'ma Zh. Eksp. Teor. Fiz. **42**, 249 (1985)].
[37]A. A. Gorokhovskii, V. Kh. Korrovits, V. V. Pal'm, and M. A. Trummal, Chem. Phys. Lett. **125**, 355 (1986).
[38]J. H. Meyling, W. H. Hesselink, and D. A. Wiersma, Chem. Phys. **17**, 353 (1976).
[39]J. H. Meyling, P. J. Bounds, and R. W. Munn, Chem. Phys. Lett. **51**, 234 (1977).
[40]U. Even and J. Jortner, J. Phys. Chem. **87**, 28 (1983).
[41]S. Jahn, Diploma thesis, University of Bayreuth, 1989.